



 Cite this: *Med. Chem. Commun.*,
2018, 9, 1529

Novel organophosphorus aminopyrimidines as unique structural DNA-targeting membrane active inhibitors towards drug-resistant methicillin-resistant *Staphylococcus aureus*†

 Di Li, Rammohan R. Yadav Bheemanaboina,‡ Narsaiah Battini,‡
Vijai Kumar Reddy Tangadanchu,§ Xian-Fu Fang and Cheng-He Zhou *

A series of novel unique structural organophosphorus aminopyrimidines were developed as potential DNA-targeting membrane active inhibitors through an efficient one-pot procedure from aldehydes, phosphonate and aminopyrimidine. The biological assay revealed that some of the prepared compounds displayed antibacterial activities. In particular, imidazole derivative **2c** exhibited more potent inhibitory activity against MRSA with an MIC value of 4 $\mu\text{g mL}^{-1}$ in comparison with the clinical drugs chloromycin and norfloxacin. Experiments revealed that the active molecule **2c** had the ability to rapidly kill the tested strains without obviously triggering the development of bacterial resistance, showed low toxicity to L929 cells and could disturb the cell membrane. The molecular docking study discovered that compound **2c** could bind with DNA gyrase *via* hydrogen bonds and other weak interactions. Further exploration disclosed that the active molecule **2c** could also effectively intercalate into MRSA DNA and form a steady **2c**-DNA supramolecular complex, which might further block DNA replication to exert powerful antibacterial effects.

 Received 15th June 2018,
Accepted 29th July 2018

DOI: 10.1039/c8md00301g

rsc.li/medchemcomm

1. Introduction

The aggravating bacterial resistance against currently available antibiotics and the lack of new antibiotics have become a major challenge in the treatment of infectious diseases. Methicillin-resistant *Staphylococcus aureus* (MRSA) is one of the most threatening drug-resistant bacteria, and often causes an epidemic and outbreak of infection owing to its rapid propagation and multi-drug resistance.¹ Antibiotics approved for treatment of MRSA infections mainly include vancomycin, linezolid, dalbavancin, daptomycin, oritavancin, tedizolid and ceftaroline.² Nevertheless, the reduced susceptibility to vancomycin and the resistance to linezolid as well as daptomycin have already emerged in clinical MRSA strains.³ MRSA has been listed as one of the deadliest superbugs by the World Health Organization (WHO).⁴ Consequently, there is an ur-

gent need to develop anti-MRSA agents with a novel structure, high efficiency and low toxicity in response to drug resistance.

Aminopyrimidine is a two-nitrogen aromatic scaffold with an electron-donating NH_2 moiety and two electron-accepting $\text{C}=\text{N}$ groups. This special structure can easily interact with various biomolecules like deoxyribonucleic acid (DNA), ribonucleic acid (RNA), enzymes and receptors with high affinity *via* intermolecular supramolecular interaction, and is extensively employed to design molecules of biological or pharmaceutical interest.⁵ It is well accepted that aminopyrimidine types of derivatives are capable of inhibiting dihydrofolate reductase,⁶ which plays a significant role in DNA synthesis, to exhibit efficient antibacterial activities.⁷ The hybridization of the aminopyrimidine moiety with active structural fragments was found to endow these hybrids with membrane active potentiality.⁸ A lot of drugs with the aminopyrimidine moiety are conveniently available in the market like sulfadiazine,⁹ rosuvastatin,¹⁰ pyrimethamine¹¹ and so on. The successful development of various aminopyrimidine drugs has gained increasing interest to discover more bioactive aminopyrimidine-based drugs.¹²

Phosphorus, as an essential element in living organisms, plays an important role in biosystems. The chemistry of low valent phosphorus resembles that of carbon owing to its similar electronegativity to carbon which makes it highly

Institute of Bioorganic & Medicinal Chemistry, Key Laboratory of Applied Chemistry of Chongqing Municipality, School of Chemistry and Chemical Engineering, Southwest University, Chongqing 400715, PR China.

E-mail: zhouch@swu.edu.cn; Fax: +86 23 68254967; Tel: +86 23 68254967

† Electronic supplementary information (ESI) available. See DOI: 10.1039/c8md00301g

‡ Postdoctoral fellow from CSIR-Indian Institute of Integrative Medicine (IIIM), India.

§ Postdoctoral fellows from CSIR-Indian Institute of Chemical Technology (IICT), India.

appropriate for synthesizing compounds in biological applications.¹³ Organophosphorus functional groups may affect the reactivity of heterocycles and regulate important biological functions,¹⁴ and these compounds possess suitable binding affinities to diverse biological targets. To date, many studies have reported the biological activities of heterocycles with organophosphorus fragments,¹⁵ and demonstrated the enormous potency of organophosphorus derivatives in the antimicrobial aspect.

On the basis of the above considerations, and as a continuous extension of our focus on the development of pyrimidine derivatives¹⁶ as DNA-targeting membrane active inhibitors, it is of great interest for us to combine the aminopyrimidine and organophosphorus fragment to generate new potentially active molecules as shown in Fig. 1. The design of target compounds was varied from the aspect of different aromatic groups. Imidazole is a vital moiety for the physiological action of histamine and histidine in biological systems and its derivatives are conveniently modified by various functional groups to produce various bioactive molecules.¹⁷ It is well known that phenyl groups exist in a variety of clinical drugs and could improve the binding affinity to targets,¹⁸ thus the five-membered structure was replaced by a six-membered ring *viz.* a benzene ring with different substituents to investigate their effects on biological activity. The indole nucleus belongs to a fused ring with benzene and is extensively present in natural products. A great number of heterocycles bearing an indolyl moiety have been reported to demonstrate an effective inhibitory profile.¹⁹ Thus, the indole ring was incorporated into target molecules. Coumarin, as a medicinal fragment, has been increasingly attracting special interest due to its potential outstanding contributions to the prevention and treatment of diseases, and related research studies have become an extremely attractive highlight.²⁰ Therefore, the coumarin moiety with two six-membered rings

was used to explore the effects on biological activities as a comparison to the indole ring. Also, carbazole with three rings has a peculiar rigid structure and endows its derivatives with excellent biological activity in medicinal chemistry.²¹ Hence, various aromatic fragments were introduced into target compounds in order to evaluate their contribution to biological activities. It is verified that the alkyl chain is able to exert an advantageous effect on biological potency by regulating the lipid-water partition coefficient and binding affinity to targets, and the aliphatic chain may deeply penetrate into the lipid bilayers of cell walls to effectively permeate the membrane.²² Reasonably, different lengths of various alkyl chains were incorporated into the imidazole nucleus to investigate the effects on antimicrobial activities. Meanwhile, the phenyl moieties bearing fluoro, chloro, nitro, methyl and methoxy groups were beneficial in regulating the pharmacological properties.²³

All the new organophosphorus pyrimidines were characterized by spectral analysis and screened against microbes including drug-resistant bacteria and fungi. The most active compound was further investigated for the resistance development, bactericidal kinetic behavior, cytotoxicity, bacterial membrane permeabilization and molecular docking. The interaction of the highly active molecule with DNA isolated from sensitive bacteria was also investigated by fluorescence and UV-vis absorption spectroscopy with the aim of exploring the possible antibacterial mechanism.

2. Chemistry

An easy synthesis of target organophosphorus pyrimidines is described in Scheme 1. The target compounds 2–4 and 6–8 were economically and conveniently prepared in yields of 31.2–66.8% by one-pot synthesis *via* the Kabachnik–Fields (phospha-Mannich) reaction from commercial 2-aminopyrimidine, diethyl phosphonate and a variety of aldehydes in toluene at 115 °C. However, the *N*-substituted imidazolyl pyrimidines with more than six carbon chains were difficult for us to synthesize; the reason was not clear. Phosphonate derivatives 4a, 4e and 4f were hydrolyzed with concentrated hydrochloric acid at 80 °C to afford the corresponding phosphonic acid derivatives 5a–c with moderate yields ranging from 53.2% to 62.2%. The intermediates including *N*-substituted imidazole aldehydes, indole aldehydes, coumarin aldehyde and carbazole aldehyde were synthesized in good yields according to reported literature methods.²⁴

All the new compounds were characterized by ¹H NMR, ¹³C NMR, ³¹P NMR and HRMS spectroscopy. The NMR spectra revealed that the PCH proton of phosphonate compounds 2–4 and 6–8 appeared as a multiplet peak at 5.74–6.66 ppm, while the corresponding phosphonic acid derivatives 5a–c gave a slightly upfield signal at 5.35–6.49 ppm for PCH protons. The influence of the phosphorus atom resulted in the chemical shifts of OCH₂ protons in organophosphate pyrimidines 2–4 and 6–8 at 3.77–4.10 ppm. The characteristic peaks for the 4- and 6-position protons in all pyrimidine rings

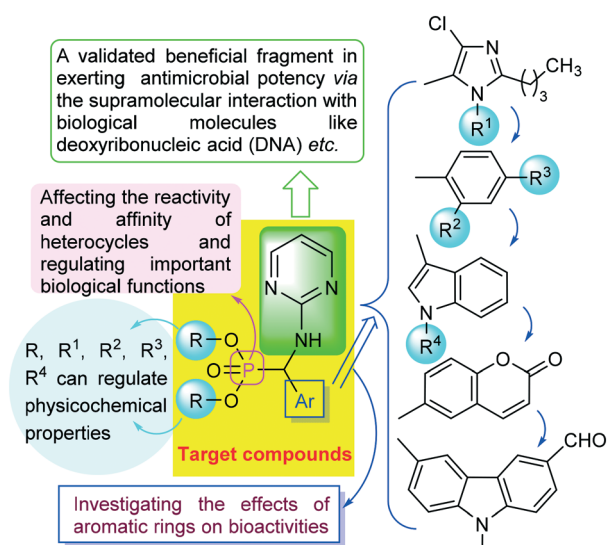
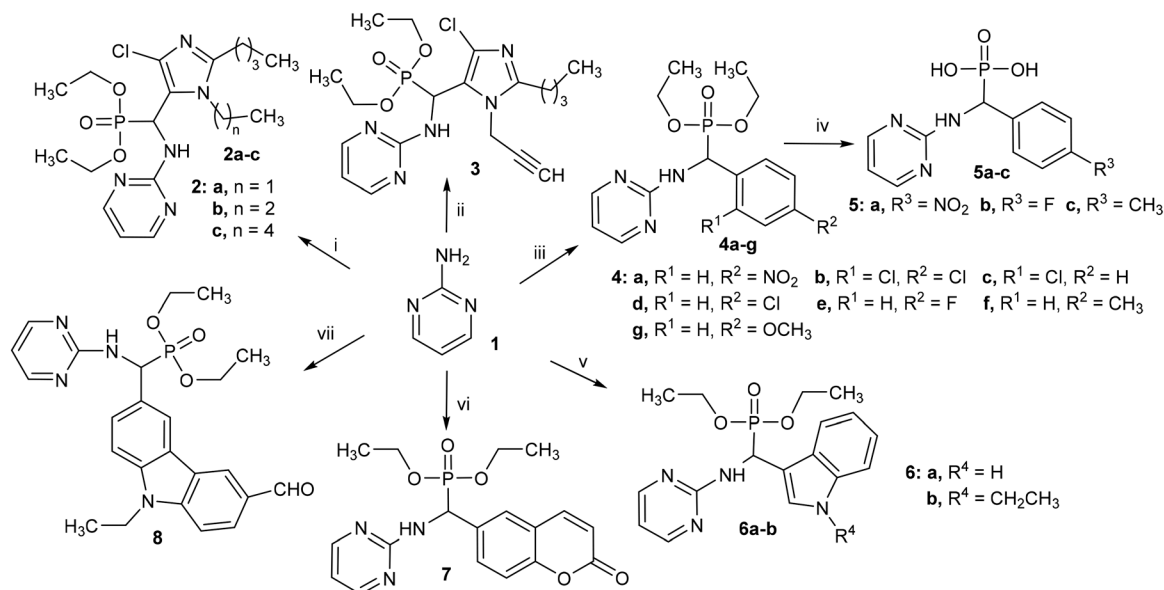


Fig. 1 Design of target organophosphorus aminopyrimidines.



Scheme 1 Reagents and conditions: (i) diethyl phosphonate, alkyl imidazole aldehyde, toluene, 115 °C, 5–6 h; (ii) diethyl phosphonate, propargyl imidazole aldehyde, toluene, 115 °C, 7 h; (iii) diethyl phosphonate, phenyl aldehyde, toluene, 115 °C, 3–5 h; (iv) conc. hydrochloric acid, 80 °C, 12 h; (v) diethyl phosphonate, indole aldehyde, toluene, 115 °C, 5–6 h; (vi) diethyl phosphonate, 2-oxo-2H-chromene-6-carbaldehyde, toluene, 115 °C, 5 h; (vii) diethyl phosphonate, 9-ethyl-9H-carbazole-3,6-dicarbaldehyde, toluene, 115 °C, 5 h.

appeared in the range of 8.21–8.57 ppm due to the electronegativity of nitrogen atoms at the 1- and 3-positions. The 5-position proton of the pyrimidine nucleus in molecules 2–8 gave an upfield signal ranging from 6.63 to 7.00 ppm. The ^{13}C NMR spectrum of target phosphate compounds 2–4 and

6–8 revealed the chemical shifts of the PCH carbons at 62.5–67.8 ppm. Interestingly, the PCH of phosphonic acid derivatives 5a–c gave upfield chemical shifts at 53.3–54.3 ppm. The carbon atoms at the 4- and 6-positions in the pyrimidine backbone gave expected signals in the range of 160.5–164.4

Table 1 *In vitro* antibacterial data for MIC ($\mu\text{g mL}^{-1}$) of pyrimidines 2–8^{a,b,c}

Comps	Gram-positive bacteria					Gram-negative bacteria					
	MRSA	S. A.	S. A. 25923	S. A. 29213	E. F.	K. P.	E. C.	E. C. 25922	P. A.	P. A. 27853	A. B.
2a	256	512	128	256	64	128	256	256	256	256	256
2b	8	256	64	128	128	64	256	128	128	128	64
2c	4	64	32	64	8	8	128	16	64	64	32
3	128	64	32	256	256	256	256	128	256	256	128
4a	128	256	8	256	32	256	256	128	256	16	128
4b	8	64	8	64	32	64	256	16	64	8	64
4c	8	128	128	128	128	32	256	64	128	128	128
4d	64	256	64	256	32	128	512	256	256	8	128
4e	256	256	64	256	64	128	256	256	128	64	128
4f	128	256	16	256	8	128	256	128	256	64	128
4g	256	256	64	256	64	256	256	256	128	4	128
5a	128	128	128	128	128	256	128	128	128	256	256
5b	128	256	128	256	256	256	256	128	256	128	256
5c	256	256	128	256	256	128	128	256	128	256	256
6a	4	256	256	128	256	64	256	256	256	256	128
6b	4	64	64	256	128	64	256	256	256	128	64
7	256	128	64	128	512	512	512	256	64	512	64
8	128	256	256	256	16	256	512	256	256	256	128
A	16	8	8	4	8	8	32	16	32	8	16
B	8	0.5	1	2	4	4	16	8	2	0.5	8

^a Minimum inhibitory concentrations (MIC, $\mu\text{g mL}^{-1}$) were determined by the microbroth dilution method for microdilution plates. ^b MRSA, methicillin-resistant *Staphylococcus aureus*; S. A., *Staphylococcus aureus*; S. A. 25923, *Staphylococcus aureus* ATCC 25923; S. A. 29213, *Staphylococcus aureus* ATCC 29213; E. F., *Enterococcus faecalis*; K. P., *Klebsiella pneumoniae*; E. C., *Escherichia coli*; E. C. 25922, *Escherichia coli* ATCC 25922; P. A., *Pseudomonas aeruginosa*; P. A. 27853, *Pseudomonas aeruginosa* ATCC 27853; A. B., *Acinetobacter baumannii*. ^c A = chloramphenicol, B = norfloxacin.

ppm. The 5-position carbon of the pyrimidine ring displayed a chemical shift at 158.4–163.4 ppm. In the ^{31}P NMR spectra, the alkyl imidazole derivatives 2a–c gave a phosphorus singlet at about 19.5 ppm, and the substitution of the propyl moiety by the propargyl group resulted in a downfield phosphorus chemical shift at 22.2 ppm for compound 3. In comparison with alkyl imidazole derivatives 2a–c, all the phenyl derivatives 4a–g gave a downfield signal at 20.5–22.3 ppm. However, when the ethyl group was removed from phosphates 4a, 4e and 4f, the corresponding phosphonic acids 5a–c gave upfield peaks for phosphorus NMR signals at 15.2–17.3 ppm. The obtained HRMS data were in very good agreement with the assigned structures. Some representative spectra are provided in the ESI.†

3. Results and discussion

3.1 Biological activity

3.1.1 Antibacterial activities. All the synthesized organophosphorus pyrimidines were evaluated for their antimicrobial activities *in vitro*. The obtained results as depicted in Table 1 showed that most of the prepared compounds exhibited antibacterial activity against the tested strains.

The length of the alkyl chain was found to affect the antibacterial activity; the introduction of an alkyl chain in imidazole aldehyde yielded target compounds 2a–c with weak to good inhibitory activity. With the increase of the alkyl chain length, compound 2b exerted equivalent or superior anti-MRSA activity with an MIC value of $8\ \mu\text{g mL}^{-1}$ to norfloxacin ($\text{MIC} = 8\ \mu\text{g mL}^{-1}$) and chloromycin ($\text{MIC} = 16\ \mu\text{g mL}^{-1}$). Notably, molecule 2c gave broad spectrum and better antibacterial activities in comparison with the other alkyl ones, especially towards Gram-positive bacteria MRSA, *Enterococcus faecalis* and Gram-negative bacteria *Klebsiella pneumonia* with MIC values of 4, 8 and $8\ \mu\text{g mL}^{-1}$, respectively, which displayed comparable or even superior inhibitory activities to standard drugs chloromycin and norfloxacin. These results preliminarily demonstrated that the increase of the alkyl chain length was favorable for bioactivity. The poor lipophilicity of imidazolyl organophosphorus pyrimidines with short alkyl chains might make them difficult to be delivered to the binding sites and result in weak antibacterial effects. Regrettably, target compounds with longer carbon chains at the *N*-imidazole ring were not obtained in our synthesis, and more work will be necessary to explore the effects of longer carbon chains on biological activities.

The substitution of the propyl group by the propargyl moiety in imidazole 2b resulted in decreased activities for propargyl imidazole derivative 3 against most of the standard strains, except for *Staphylococcus aureus* and *Staphylococcus aureus* ATCC 25923. In particular, compound 3 gave a lower anti-MRSA potency ($\text{MIC} = 128\ \mu\text{g mL}^{-1}$), 16-fold less potent than molecule 2b ($\text{MIC} = 8\ \mu\text{g mL}^{-1}$). These studies disclosed that the propargyl group was not conducive to antibacterial activities.

In comparison with the organophosphorus imidazole pyrimidine 2, some of the phenyl ones 4a–g exerted comparable or even superior inhibitory activities against some of the tested bacteria. The antibacterial potency of 4-nitrophenyl compound 4a towards *Staphylococcus aureus* ATCC 25923 was equivalent to the reference drug chloromycin ($\text{MIC} = 8\ \mu\text{g mL}^{-1}$). It was noteworthy that 2,4-dichlorophenyl compound 4b showed a broad antibacterial spectrum and good activities with MIC values of $8\text{--}32\ \mu\text{g mL}^{-1}$ against MRSA, *Staphylococcus aureus* ATCC 25923, *Enterococcus faecalis*, *Escherichia coli* ATCC 25922 and *Pseudomonas aeruginosa* ATCC 27853. In particular, it was observed that 2-chlorophenyl compound 4c exhibited better anti-MRSA activity with an MIC value of $8\ \mu\text{g mL}^{-1}$ than chloromycin ($\text{MIC} = 16\ \mu\text{g mL}^{-1}$), and 4-chlorophenyl molecule 4d was effective in inhibiting the growth of Gram-negative bacteria *Pseudomonas aeruginosa* ATCC 27853 at low concentrations ($\text{MIC} = 8\ \mu\text{g mL}^{-1}$). Moreover, 4-methylphenyl derivative 4f could inhibit the growth of *Enterococcus faecalis* with an MIC value of $8\ \mu\text{g mL}^{-1}$. Noticeably, 4-methoxyphenyl derivative 4g showed better anti-*Pseudomonas aeruginosa* ATCC 27853 activity with a MIC value of $4\ \mu\text{g mL}^{-1}$, which was superior to the standard drug chloromycin ($\text{MIC} = 8\ \mu\text{g mL}^{-1}$). These results suggested that a chloro atom at the *ortho*-position on the phenyl moiety was beneficial for the biological activities towards MRSA and a chloro atom at the *para*-position on the phenyl moiety was more helpful for the inhibition of the *Pseudomonas aeruginosa* ATCC 27853 strain. However, the hydrolyzed pyrimidines 5a–c showed nearly no significant inhibitory potential against any of the tested bacteria with MIC values greater than $128\ \mu\text{g mL}^{-1}$.

Indolyl aminopyrimidines 6a and 6b displayed superior antibacterial efficacies against MRSA, both with MIC values of $4\ \mu\text{g mL}^{-1}$, to chloromycin ($\text{MIC} = 16\ \mu\text{g mL}^{-1}$) and norfloxacin ($\text{MIC} = 8\ \mu\text{g mL}^{-1}$), but gave fairly poor antibacterial potencies with MIC values in the range of $64\text{--}256\ \mu\text{g mL}^{-1}$ towards the other bacterial strains. Coumarin derivative 7 exhibited decreased activities in comparison with the indolyl one 6. Furthermore, carbazole compound 8 displayed weak to moderate bioactivity, except for anti-*Enterococcus faecalis* activity ($\text{MIC} = 16\ \mu\text{g mL}^{-1}$). These results suggested that the enlargement of the aromatic structures was unfavorable for the bioactivities of the target compounds.

3.1.2 Antifungal activities. The antifungal evaluation *in vitro* revealed that most of the target compounds showed inferior antifungal efficiency in comparison with fluconazole, except for *Aspergillus fumigatus* as shown in Table S1.† Among these pyrimidine derivatives 2–8, the phenyl derivatives 4a–g gave weak to good inhibitory potentiality against *Aspergillus fumigatus* with MIC values greater than $16\ \mu\text{g mL}^{-1}$, which gave 16-fold more potent antifungal efficacy than the reference drug fluconazole ($\text{MIC} = 256\ \mu\text{g mL}^{-1}$). Noticeably, *Candida albicans* ATCC 90023 was sensitive to compounds 4b and 4d with a MIC value of $8\ \mu\text{g mL}^{-1}$; this might suggest that a chloro atom at the *para*-position of the phenyl ring exhibited a positive effect in inhibiting the growth of *Candida albicans* ATCC 90023.

3.2 Resistance study

MRSA has become one of the most challenging nosocomial pathogens in clinics due to the emergence and contagion of antibiotic resistance.²⁵ It is extremely significant to investigate the propensity of novel promising drug candidates for inducing bacterial resistance. Consequently, the drug resistance study of the active molecule **2c** towards MRSA was done, and clinical antibacterial norfloxacin was used as a positive control. As shown in Fig. 2, it is more difficult for MRSA to develop resistance to the active compound **2c** in comparison with the clinical drug norfloxacin even after 16 passages, and it was observed that there was no obvious triggering of the development of bacterial resistance for the active molecule **2c**.

3.3 Bactericidal kinetic assay

It is urgent to discover rapidly and efficiently antibacterial agents to overcome bacterial resistance.²⁶ A time-kill kinetics assay of the highly active molecule **2c** towards the MRSA strain was carried out to identify the antibacterial potency of the synthesized compound.²⁷ Fig. 3 shows that compound **2c** exhibited more than 3 log (CFU mL⁻¹) reduction in the number of viable bacteria within one hour at a concentration of 6 × MIC. Therefore, it could be interpreted that compound **2c** had a rapid killing effect against the MRSA strain.

3.4 Cytotoxicity

Cytotoxicity is one of the most essential criteria to screen potential bioactive molecules.²⁸ The active molecule **2c** was further examined for its cytotoxic properties against normal mouse fibroblast L929 cells (Boster Biological Technology Co. Ltd, Tianjin, China). Fig. 4 shows the *in vitro* cytotoxicity of compound **2c** against L929 cells which was evaluated by the MTT assay. As shown in Fig. 4, the cell viability of pyrimidine **2c** towards L929 cells was at least 80% within the concentration of 128 μg mL⁻¹, and it revealed that compound **2c** displayed relatively low toxicity to L929 cells within the MIC values.

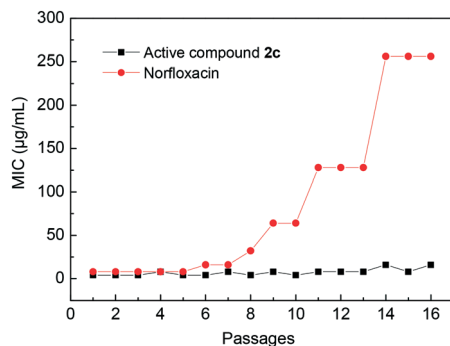


Fig. 2 Drug resistance test for the active molecule **2c** towards the MRSA strain.

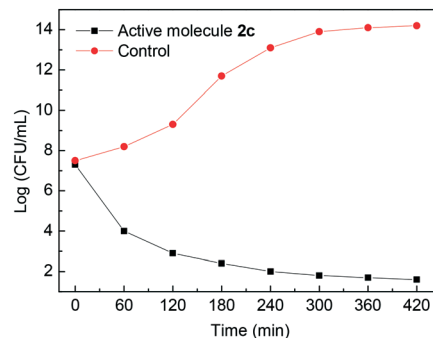


Fig. 3 Time-kill kinetics of the active molecule **2c** (6 × MIC) against MRSA.

3.5 Bacterial membrane permeabilization

The bacterial membrane, as a significant and intriguing antibacterial target, has been studied. Propidium iodide (PI) dye is a fluorescent dye used to detect the ability of biocides to permeabilize the cytoplasmic membrane of bacteria.²⁹ This dye can pass through the membrane of compromised bacterial cells and fluoresces upon binding to the DNA.³⁰ In Fig. 5, the rapid fluorescence intensity enhancements of the mixtures of compound **2c** and PI-treated MRSA appeared and became steady after 70 min; this illustrated that the tested compound **2c** could efficiently interfere with the membranes of MRSA.

3.6 Molecular docking

To further gain insight into the binding interactions of these organophosphorus pyrimidines, docking studies were then carried out to examine the docking pose of compound **2c** into the gyrase–DNA complex. The crystal structure data was obtained from the protein data bank (PDB code: 2XCS), which was a representative target used to investigate the antibacterial mechanism.³¹ Fig. 6 and S1 (ESI†) revealed the supramolecular interaction of compound **2c** with the gyrase–DNA receptor. It is reasonable to explain the possible antibacterial mechanism of the interaction between imidazole **2c** and the gyrase–DNA complex by this docking result. The docking mode gave the lowest binding energy values of -9.55 kcal mol⁻¹ (*R*-enantiomer) and -7.63 kcal mol⁻¹ (*S*-enantiomer), which indicated that the *R*-enantiomer of

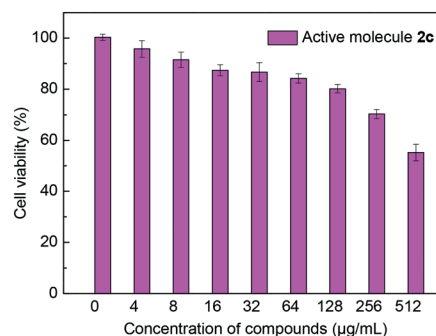


Fig. 4 Relative cell viabilities of the active molecule **2c** in L929 cells.

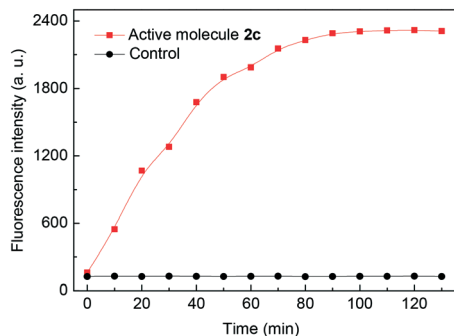


Fig. 5 Bacterial membrane permeabilization of compound 2c (12 × MIC) against the MRSA strain.

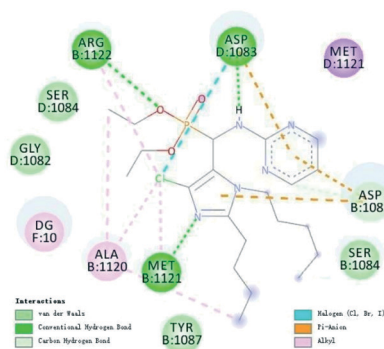


Fig. 6 Supramolecular binding of compound 2c docked in the bacterial DNA-gyrase complex (PDB code: 2XCS).

molecule 2c was a more favorable stereoisomer in inhibiting the function of DNA gyrase. As shown in Fig. 6, the hydrogen atom of the NH group at the 2-position on aminopyrimidine was in close proximity to the ASP1083 residue of gyrase through two hydrogen bonds with a distance of 1.9 Å, which illustrated the necessity of the NH group for increased bioactivity. Meanwhile, other two hydrogen bonds were formed by compound 2c with the ASP1083 residue through the oxygen atom of the OCH₂CH₃ fragment and the nitrogen atom of the imidazole ring. Furthermore, electrostatic interactions existed between the aromatic ring and imidazolyl fragments of compound 2c and residues MET1121, ASP1083, ALA1120 and ARG1122 in DNA gyrase. All of these cooperative bindings might be beneficial in stabilizing the 2c-enzyme-DNA supramolecular complex, which might be responsible for the good inhibitory efficacy of compound 2c against the tested strains.

3.7 Interactions of the active molecule 2c with MRSA DNA

Bacterial DNA, as a selected therapeutic target, has drawn increasing attention in finding potent antibacterial agents due to its function of encoding genetic instructions.³² The pyrimidine nucleus can interact with DNA, thus it is of interest for us to explore the possible antimicrobial action mechanism. Thus, MRSA DNA was isolated from MRSA strains and its binding behavior with the active molecule 2c was investigated at the molecular level *in vitro* using neutral red (NR) dye as a spectral probe by UV-vis absorption spectroscopy.

3.7.1 Absorption spectra of MRSA DNA in the presence of the active molecule 2c. Absorption spectroscopy plays a vital role in DNA-binding studies.³³ Due to the stacking interaction between an aromatic chromophore and the base pairs of DNA, the absorbance spectrum will show hyperchromism and hypochromism when a compound binds to DNA. With a fixed concentration of DNA, UV-vis absorption spectra were recorded with successively increasing amount of the active compound 2c. The inset in Fig. 7 shows that the absorption peak of DNA at 260 nm exhibits a gradual increase and slight red shift with increasing concentration of compound 2c. Furthermore, the measured absorption values of the simple sum of free DNA and free compound 2c were obviously higher than that of the DNA-2c complex, which illustrated that a hypochromic effect existed between MRSA DNA and molecule 2c. According to the values from the UV-vis spectra, pyrimidine 2c could actually interact with MRSA DNA, and thus the binding mode of compound 2c with MRSA DNA deserved to be further investigated.

On the basis of the variations in the absorption spectra of MRSA DNA upon binding to molecule 2c, eqn (1)³⁴ can be utilized to calculate the binding constant (K):

$$\frac{A^0}{A^0 - A} = \frac{\xi_C}{\xi_{D-C} - \xi_C} + \frac{\xi_C}{\xi_{D-C} - \xi_C} \times \frac{1}{K[Q]} \quad (1)$$

where A^0 and A represent the absorbance of MRSA DNA at 260 nm in the absence and presence of compound 2c, and ξ_C and ξ_{D-C} are the absorption coefficients of compound 2c and the DNA-2c complex, respectively. The plot of $A^0/(A - A^0)$ versus $1/[\text{compound 2c}]$ is constructed by using the absorption titration data and linear fitting in Fig. 8, yielding the binding constant, $K = 6.84 \times 10^3 \text{ L mol}^{-1}$, $R = 0.9989$, $SD = 0.0280$ (R is the correlation coefficient, and SD is the standard deviation).

3.7.2 Absorption spectra of NR interaction with MRSA DNA. Neutral red (NR) is a planar phenazine dye and is

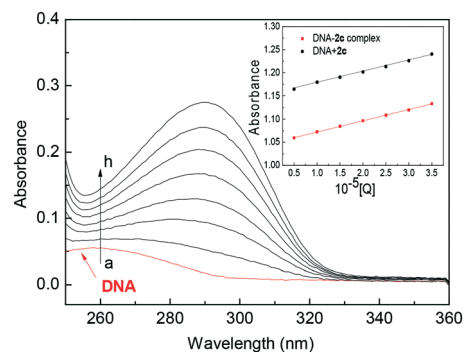


Fig. 7 UV absorption spectra of MRSA DNA with different concentrations of compound 2c (pH = 7.4, $T = 287 \text{ K}$). Inset: Comparison of absorption at 260 nm of the 2c-DNA complex and the sum values of free DNA and free compound 2c. $c(\text{DNA}) = 7.44 \times 10^{-5} \text{ mol L}^{-1}$, and $c(\text{compound 2c}) = 0-3.50 \times 10^{-5} \text{ mol L}^{-1}$ for curves a-h, respectively, at an increment of 0.5×10^{-5} .

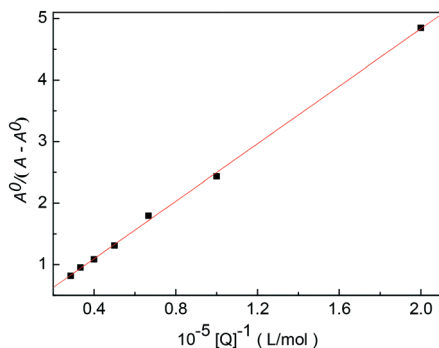


Fig. 8 The plot of $A^0/(A - A^0)$ versus $1/[\text{compound } 2c]$.

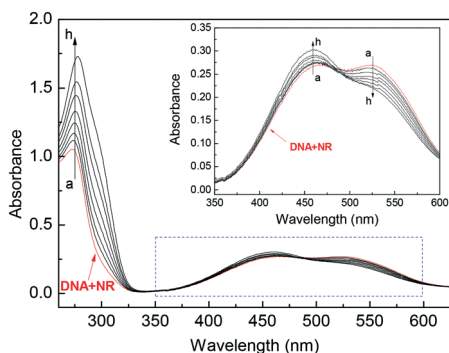


Fig. 9 UV absorption spectra of the competitive reaction between compound 2c and NR with MRSA DNA. $c(\text{DNA}) = 7.44 \times 10^{-5} \text{ mol L}^{-1}$, $c(\text{NR}) = 2 \times 10^{-5} \text{ mol L}^{-1}$, and $c(\text{compound } 2c) = 0\text{--}3.50 \times 10^{-5} \text{ mol L}^{-1}$ for curves a–h, respectively, at an increment of 0.5×10^{-5} . Inset: Absorption spectra of the system with increasing concentration of compound 2c in the wavelength range of 350–600 nm and absorption spectra of the competitive reaction between compound 2c and NR with DNA.

structurally similar to other planar dyes like acridine, thiazine and xanthene;³⁵ it possesses the following advantages: low toxicity, high stability and convenient application.³⁶ It has been shown that the binding mode of NR with DNA is of the intercalative binding type by spectrophotometric and electrochemical techniques. Therefore, NR was used as a spectral probe to study the binding mode of molecule 2c with MRSA DNA in this work. As shown in Fig. S2 (ESI[†]), a gradual decrease with increasing concentration of MRSA DNA in the intensity of the absorption peak of NR around 455 nm was observed, and a new band around 530 nm was developed, which should be attributed to the formation of a new DNA–NR complex. This was further confirmed by the isosbestic point at 504 nm.

3.7.3 Absorption spectra of the competitive interaction of active molecule 2c and NR with MRSA DNA. The absorption spectra of the competitive binding between NR and compound 2c with MRSA DNA were obtained. Fig. 9 shows an obvious increase in the developing band around 455 nm, but the maximum absorption around 530 nm of the DNA–NR complex is decreased. The spectra in the inset in Fig. 9 show the reverse process in comparison with the absorption band

at around 455 nm of the free NR in the presence of increasing concentrations of MRSA DNA (Fig. S2 (ESI[†])). The results indicated that the active compound 2c intercalated into the double helix of MRSA DNA by substituting for NR in the DNA–NR complex.

4. Conclusion

In conclusion, a series of novel organophosphorus pyrimidines as unique structural DNA-targeting membrane active inhibitors were successfully synthesized through a convenient and efficient strategy from 2-aminopyrimidine, phosphonate and aromatic aldehydes. Their structures were characterized by ¹H NMR, ¹³C NMR, ³¹P NMR and HRMS spectroscopy. Some of the target molecules could selectively and effectively inhibit the growth of some of the tested strains. Imidazolyl pyrimidine 2c gave a broad antibacterial spectrum. In particular, compound 2c exhibited stronger activity against MRSA with a MIC value of $4 \mu\text{g mL}^{-1}$ in comparison with standard drugs chloramycycin and norfloxacin. Further study revealed that active compound 2c was able to disturb the cell membrane and exhibited low toxicity against L929 cells. In addition, molecule 2c could not only rapidly kill the tested strains but also effectively control the development of bacterial resistance. The molecular docking study revealed that compound 2c could bind with DNA gyrase by the formation of hydrogen bonds. This preliminary research revealed that a steady complex could be formed by intercalation of compound 2c with MRSA DNA which might be responsible for the potent bioactivity. All the results revealed that imidazolyl derivative 2c might serve as a DNA-targeting membrane active inhibitor towards MRSA strains.

Conflicts of interest

There are no conflicts to declare.

Acknowledgements

This work was partially supported by the National Natural Science Foundation of China (No. 21672173), the Research Fund for International Young Scientists from International (Regional) Cooperation and Exchange Program (No. 81350110523), the China Postdoctoral Science Foundation (2018M633313), the Chongqing Special Foundation for Postdoctoral Research Proposal (Nos. Xm2016039, Xm2017184), and the Program for Overseas Young Talents from State Administration of Foreign Experts Affairs, China (Nos. WQ2017XNDX047, WQ20180083).

Notes and references

- (a) W. Kim, W. P. Zhu, G. L. Hendricks, D. Van Tyne, A. D. Steele, C. E. Keohane, N. Fricke, A. L. Conery, S. Shen, W. Pan, K. Lee, R. Rajamuthiah, B. B. Fuchs, P. M. Vlahovska, W. M. Wuest, M. S. Gilmore, H. J. Gao, F. M. Ausubel and E. Mylonakis, *Nature*, 2018, 556, 103–107; (b) H. F. Chambers and F. R. DeLeo, *Nat. Rev. Microbiol.*, 2009, 7, 629–641.

- 2 H. Z. Zhang, L. L. Gan, H. Wang and C. H. Zhou, *Mini-Rev. Med. Chem.*, 2017, 17, 122–166.
- 3 S. M. Lehar, T. Pillow, M. Xu, L. Staben, K. K. Kajihara, R. Vandlen, L. DePalatis, H. Raab, W. L. Hazenbos, J. H. Morisaki, J. Kim, S. Park, M. Darwish, B. C. Lee, H. Hernandez, K. M. Loyet, P. Lupardus, R. Fong, D. H. Yan, C. Chalouni, E. Luis, Y. Khalfin, E. Plise, J. Cheong, J. P. Lyssikatos, M. Strandh, K. Kofoed, P. S. Andersen, J. A. Flygare, M. W. Tan, E. J. Brown and S. Mariathasan, *Nature*, 2015, 527, 323–328.
- 4 S. M. Lin, J. Koh, T. T. Aung, W. L. W. Sin, F. H. Lim, L. Wang, R. Lakshminarayanan, L. Zhou, D. T. H. Tan, D. R. Cao, R. W. Beuerman, L. Ren and S. P. Liu, *J. Med. Chem.*, 2017, 60, 6152–6165.
- 5 (a) A. C. Borisa and H. G. Bhatt, *Eur. J. Med. Chem.*, 2017, 140, 1–19; (b) M. Uria-Nickelsen, G. Neckermann, S. Sriram, B. Andrews, J. I. Manchester, D. Carcanague, S. Stokes and K. G. Hull, *Int. J. Antimicrob. Agents*, 2013, 41, 363–371.
- 6 B. Nammalwar, R. A. Bunce, K. D. Berlin, C. R. Bourne, P. C. Bourne, E. W. Barrow and W. W. Barrow, *Eur. J. Med. Chem.*, 2012, 54, 387–396.
- 7 H. B. Liu, W. W. Gao, V. K. R. Tangadanchu, C. H. Zhou and R. X. Geng, *Eur. J. Med. Chem.*, 2018, 143, 66–84.
- 8 L. R. Odell, M. K. Abdel-Hamid, T. A. Hill, N. Chau, K. A. Young, F. M. Deane, J. A. Sakoff, S. Andersson, J. A. Daniel, P. J. Robinson and A. McCluskey, *J. Med. Chem.*, 2017, 60, 349–361.
- 9 J. J. Hogan, G. S. Markowitz and J. Radhakrishnan, *Clin. J. Am. Soc. Nephrol.*, 2015, 10, 1300–1310.
- 10 M. M. Abdel-Daim and A. Abdeen, *Food Chem. Toxicol.*, 2018, 114, 69–77.
- 11 J. Gallay, S. Prod'hom, T. Mercier, C. Bardinnet, D. Spaggiari, E. Pothin, T. Buclin, B. Genton and L. A. Decosterd, *J. Pharm. Biomed. Anal.*, 2018, 154, 263–277.
- 12 (a) A. P. Mehta, H. Li, S. A. Reed, L. Supekova, T. Javahishvili and P. G. Schultz, *J. Am. Chem. Soc.*, 2016, 138, 14230–14233; (b) C. E. Powell, Y. Gao, L. Tan, K. A. Donovan, R. P. Nowak, A. Loehr, M. Bahcall, E. S. Fischer, P. A. Jänne, R. E. George and N. S. Gray, *J. Med. Chem.*, 2018, 61, 4249–4255.
- 13 S. M. Engel, A. Bradman, M. S. Wolff, V. A. Rauh, K. G. Harley, J. H. Yang, L. A. Hoepner, D. B. Barr, K. Yolton, M. G. Vedar, Y. Y. Xu, R. W. Hornung, J. G. Wetmur, J. Chen, N. T. Holland, F. P. Perera, R. M. Whyatt, B. P. Lanphear and B. Eskenazi, *Environ. Health Perspect.*, 2016, 124, 822–830.
- 14 C. Alonso, M. Fuertesa, E. Martín-Encinasa, A. Selas, G. Rubiales, C. Tesauero, B. K. Knudssen and F. Palacios, *Eur. J. Med. Chem.*, 2018, 149, 225–237.
- 15 (a) W. S. Huang, S. Liu, D. Zou, M. Thomas, Y. Wang, T. Zhou, J. Romero, A. Kohlmann, F. Li, J. Qi, L. Cai, T. A. Dwight, Y. Xu, R. Xu, R. Dodd, A. Toms, L. Parillon, X. Lu, R. Anjum, S. Zhang, F. Wang, J. Keats, S. D. Wardwell, Y. Ning, Q. Xu, L. E. Moran, Q. K. Mohemmad, H. G. Jang, T. Clackson, N. I. Narasimhan, V. M. Rivera, X. Zhu, D. Dalgarno and W. C. Shakespeare, *J. Med. Chem.*, 2016, 59, 4948–4964; (b) G. Németh, Z. Greff, A. Sipos, Z. Varga, R. Székely, M. Sebestyén, Z. Jászay, S. Béni, Z. Nemes, J. Pirat, J. Volle, D. Virieux, Á. Gyuris, K. Kelemenics, É. Áy, J. Minarovits, S. Szathmary, G. Kéri and L. Órfi, *J. Med. Chem.*, 2014, 57, 3939–3965; (c) W. W. Gao, S. Rasheed, V. K. R. Tangadanchu, Y. Sun, X. M. Peng, Y. Cheng, F. X. Zhang, J. M. Lin and C. H. Zhou, *Sci. China: Chem.*, 2017, 60, 769–785.
- 16 (a) X. F. Fang, D. Li, V. K. R. Tangadanchu, L. Gopala, W. W. Gao and C. H. Zhou, *Bioorg. Med. Chem. Lett.*, 2017, 27, 4964–4969; (b) X. J. Fang, P. Jeyakkumar, S. R. Avula, Q. Zhou and C. H. Zhou, *Bioorg. Med. Chem. Lett.*, 2016, 26, 2584–2588.
- 17 (a) X. M. Peng, G. X. Cai and C. H. Zhou, *Curr. Top. Med. Chem.*, 2013, 13, 1963–2010; (b) L. Zhang, K. V. Kumar, R. X. Geng and C. H. Zhou, *Bioorg. Med. Chem. Lett.*, 2015, 25, 3699–3705.
- 18 (a) S. Pospisilova, H. Michnova, T. Kauerova, K. Pauk, P. Kollar, J. Vinsova, A. Imramovsky, A. Cizek and J. Jampile, *Bioorg. Med. Chem. Lett.*, 2018, 28, 2184–2188; (b) W. W. Gao, L. Gopala, R. R. Y. Bheemanaboina, G. B. Zhang, S. Li and C. H. Zhou, *Eur. J. Med. Chem.*, 2018, 146, 15–37; (c) P. Jeyakkumar, H. B. Liu, L. Gopala, Y. Cheng, X. M. Peng, R. X. Geng and C. H. Zhou, *Bioorg. Med. Chem. Lett.*, 2017, 27, 1737–1743.
- 19 (a) S. Dadashpour and S. Emami, *Eur. J. Med. Chem.*, 2018, 150, 9–29; (b) Z. Z. Li, L. Gopala, V. K. R. Tangadanchu, W. W. Gao and C. H. Zhou, *Bioorg. Med. Chem.*, 2017, 25, 6511–6522.
- 20 X. M. Peng, G. L. V. Damu and C. H. Zhou, *Curr. Pharm. Des.*, 2013, 19, 3884–3930.
- 21 (a) Y. Zhang, V. K. R. Tangadanchu, Y. Cheng, R. G. Yang, J. M. Lin and C. H. Zhou, *ACS Med. Chem. Lett.*, 2018, 9, 244–249; (b) Y. Zhang, V. K. R. Tangadanchu, R. R. Y. Bheemanaboina, Y. Cheng and C. H. Zhou, *Eur. J. Med. Chem.*, 2018, 155, 579–589; (c) D. Addla, S. Q. Wen, S. K. Maddili, L. Zhang and C. H. Zhou, *Med. Chem. Commun.*, 2016, 7, 1988–1994; (d) F. F. Zhang, L. L. Gan and C. H. Zhou, *Bioorg. Med. Chem. Lett.*, 2010, 20, 1881–1884.
- 22 (a) H. Z. Zhang, J. M. Lin, S. Rasheed and C. H. Zhou, *Sci. China: Chem.*, 2014, 57, 807–822; (b) J. Kang, V. K. R. Tangadanchu, L. Gopala, W. W. Gao, Y. Cheng, H. B. Liu, R. X. Geng, S. Li and C. H. Zhou, *Chin. Chem. Lett.*, 2017, 28, 1369–1374.
- 23 (a) L. Zhang, K. V. Kumar, S. Rasheed, S. L. Zhang, R. X. Geng and C. H. Zhou, *Med. Chem. Commun.*, 2015, 6, 1303–1310; (b) H. Z. Zhang, S. C. He, Y. J. Peng, H. J. Zhang, L. Gopala, V. K. R. Tangadanchu, L. L. Gan and C. H. Zhou, *Eur. J. Med. Chem.*, 2017, 136, 165–183.
- 24 (a) A. Jallapally, D. Addla, P. Yogeewari, D. Sriram and S. Kantevari, *Bioorg. Med. Chem. Lett.*, 2014, 24, 5520–5524; (b) Y. L. Zhang, Y. J. Qin, D. J. Tang, M. R. Yang, B. Y. Li, Y. T. Wang, H. Y. Cai, B. Z. Wang and H. L. Zhu, *ChemMedChem*, 2016, 11, 1–14; (c) S. C. Bhunia, G. C. Patra and S. C. Pal, *Synth. Commun.*, 2011, 41, 3678–3682; (d) G. C. Zheng, Z. B.

- Cai, Y. L. Pan, L. Bai, Y. T. Zhou, S. L. Li and Y. P. Tian, *Tetrahedron*, 2016, 72, 2988–2996.
- 25 (a) H. H. Gong, K. Baathulaa, J. S. Lv, G. X. Cai and C. H. Zhou, *Med. Chem. Commun.*, 2016, 7, 924–931; (b) W. W. Gao and C. H. Zhou, *Future Med. Chem.*, 2017, 9, 1461–1464; (c) J. Kang, L. Gopala, V. K. R. Tangadanchu, W. W. Gao and C. H. Zhou, *Future Med. Chem.*, 2018, 10, 711–724.
- 26 L. Zhang, D. Addla, J. Ponmani, A. Wang, D. Xie, Y. N. Wang, S. L. Zhang, R. X. Geng, G. X. Cai, S. Li and C. H. Zhou, *Eur. J. Med. Chem.*, 2016, 111, 160–182.
- 27 P. Picconi, C. Hind, S. Jamshidi, K. Nahar, M. Clifford, M. E. Wand, J. M. Sutton and K. M. Rahman, *J. Med. Chem.*, 2017, 60, 6045–6059.
- 28 (a) S. F. Cui, D. Addla and C. H. Zhou, *J. Med. Chem.*, 2016, 59, 4488–4510; (b) Y. Cheng, S. R. Avula, W. W. Gao, D. Addla, V. K. R. Tangadanchu, L. Zhang, J. M. Lin and C. H. Zhou, *Eur. J. Med. Chem.*, 2016, 124, 935–945; (c) Y. N. Wang, R. R. Y. Bheemanaboina, G. X. Cai and C. H. Zhou, *Bioorg. Med. Chem. Lett.*, 2018, 28, 1621–1628; (d) G. B. Zhang, S. K. Maddili, V. K. R. Tangadanchu, L. Gopala, W. W. Gao, G. X. Cai and C. H. Zhou, *Sci. China: Chem.*, 2018, 61, 557–568.
- 29 M. M. Konai, C. Ghosh, V. Yarlagadda, S. Samaddar and J. Haldar, *J. Med. Chem.*, 2014, 57, 9409–9423.
- 30 (a) J. Hoque, M. M. Konai, S. Gonuguntla, G. B. Manjunath, S. Samaddar, V. Yarlagadda and J. Haldar, *J. Med. Chem.*, 2015, 58, 5486–5500; (b) P. Jeyakkumar, L. Zhang, S. R. Avula and C. H. Zhou, *Eur. J. Med. Chem.*, 2016, 122, 205–215.
- 31 (a) Y. Y. Chen, L. Gopala, R. R. Y. Bheemanaboina, H. B. Liu, Y. Cheng, R. X. Geng and C. H. Zhou, *ACS Med. Chem. Lett.*, 2017, 8, 1331–1335; (b) J. R. Duan, H. B. Liu, P. Jeyakkumar, L. Gopala, S. Li, R. X. Geng and C. H. Zhou, *Med. Chem. Commun.*, 2017, 17, 907–916.
- 32 (a) Y. L. Li, J. W. Schroeder, L. A. Simmons and J. S. Biteen, *Curr. Opin. Microbiol.*, 2018, 43, 38–45; (b) B. T. Yin, C. Y. Yan, X. M. Peng, S. L. Zhang, S. Rasheed, R. X. Geng and C. H. Zhou, *Eur. J. Med. Chem.*, 2014, 71, 148–159.
- 33 M. B. Ismail, I. N. Booyesen and M. P. Akerman, *Inorg. Chim. Acta*, 2018, 477, 257–269.
- 34 (a) S. Q. Wen, P. Jeyakkumar, S. R. Avula, L. Zhang and C. H. Zhou, *Bioorg. Med. Chem. Lett.*, 2016, 26, 2768–2773; (b) Y. N. Wang, R. R. Y. Bheemanaboina, W. W. Gao, J. Kang, G. X. Cai and C. H. Zhou, *ChemMedChem*, 2018, 13, 1004–1017.
- 35 (a) Y. Zhang, G. L. V. Damu, S. F. Cui, J. L. Mi, V. K. R. Tangadanchu and C. H. Zhou, *Med. Chem. Commun.*, 2017, 8, 1631–1639; (b) X. M. Peng, L. P. Peng, A. S. Rao, K. V. Kumar, S. Li and C. H. Zhou, *Future Med. Chem.*, 2016, 8, 1927–1940; (c) S. K. Maddili, Z. Z. Li, V. K. Kannekanti, R. R. Y. Bheemanaboina, B. Tuniki, V. K. R. Tangadanchu and C. H. Zhou, *Bioorg. Med. Chem. Lett.*, 2018, 28, 2426–2431.
- 36 (a) X. M. Peng, K. V. Kumar, G. L. V. Damu and C. H. Zhou, *Sci. China: Chem.*, 2016, 59, 878–894; (b) M. N. Shinde, R. Khurana, N. Barooah, A. C. Bhasikuttan and J. Mohanty, *Org. Biomol. Chem.*, 2017, 15, 3975–3984.